LOAD-CARRYING CAPACITY OF PRESTRESSED HOLLOW CORE SLABS

Matti Pajari
Technical Research Centre of Finland

A design method based on the true failure mechanisms of the prestressed hollow core slabs is introduced. 340 full scale load tests have been analysed and the calculated results have been compared to the experimental ones. It is concluded that the design against the shear compression failure mode can be replaced by the design against the anchorage failure mode. The modulus of rupture of concrete seems to be insensitive to the thickness of the slab. It is also smaller for the hollow core slabs than for the rectangular beams made of plain concrete. Furthermore, the shear capacity of the thick slabs may be overestimated if the tensile strength of concrete is supposed to be the same in the web as on the top of the slab.

Key words: Load-carrying capacity, prestressing, hollow core slabs, shear capacity, cracking

1. INTRODUCTION

Design of the extruded prestressed hollow core slabs has been and is largely still based on formulae developed for the reinforced concrete beams. However, the large hollows, the lack of shear reinforcement and the anchorage of the strands at the end of the slab make a considerable difference between these two products. In a sense, a prestressed hollow core slab resembles more a steel I-beam than a reinforced concrete beam.

There are few research reports dealing theoretically with the load-carrying capacity of the prestressed hollow core slabs. Jonsson /1/ has carried out numerous tests the results of which he has used for developing a simple formula for predicting the shear capacity of 265 mm slabs. Sarja and Nykyri /2/ have introduced a rotational model for the shear capacity. Walraven and Mercx have reported about extensive experimental and theoretical research concerning the bearing capacity of the prestressed hollow core slabs /3/. Becker and Buettner /4/ have applied the ACI design method /5/ to experimental data and con-cluded that this method gives capacities that are on the safe side.

The design method described in this paper was developed at Technical Research Centre of Finland during 1981 ... 1983. The object was to write a computer code for the design of the prestressed hollow core slabs. The calculation of the shear capacity was the main problem because the existing design methods were regarded unsatisfactory. Attempts were made to model the real failure mechanisms instead of fitting curves in experimental data.

2. LIMIT STATES AND THEIR MECHANICAL MODELLING

When simply supported prestressed hollow core slabs are loaded, a number of different failure mechanisms can be observed. In addition, excessive displacements and cracking at serviceability limit state must be prevented. The relevant limit states are illustrated in Fig. 1.

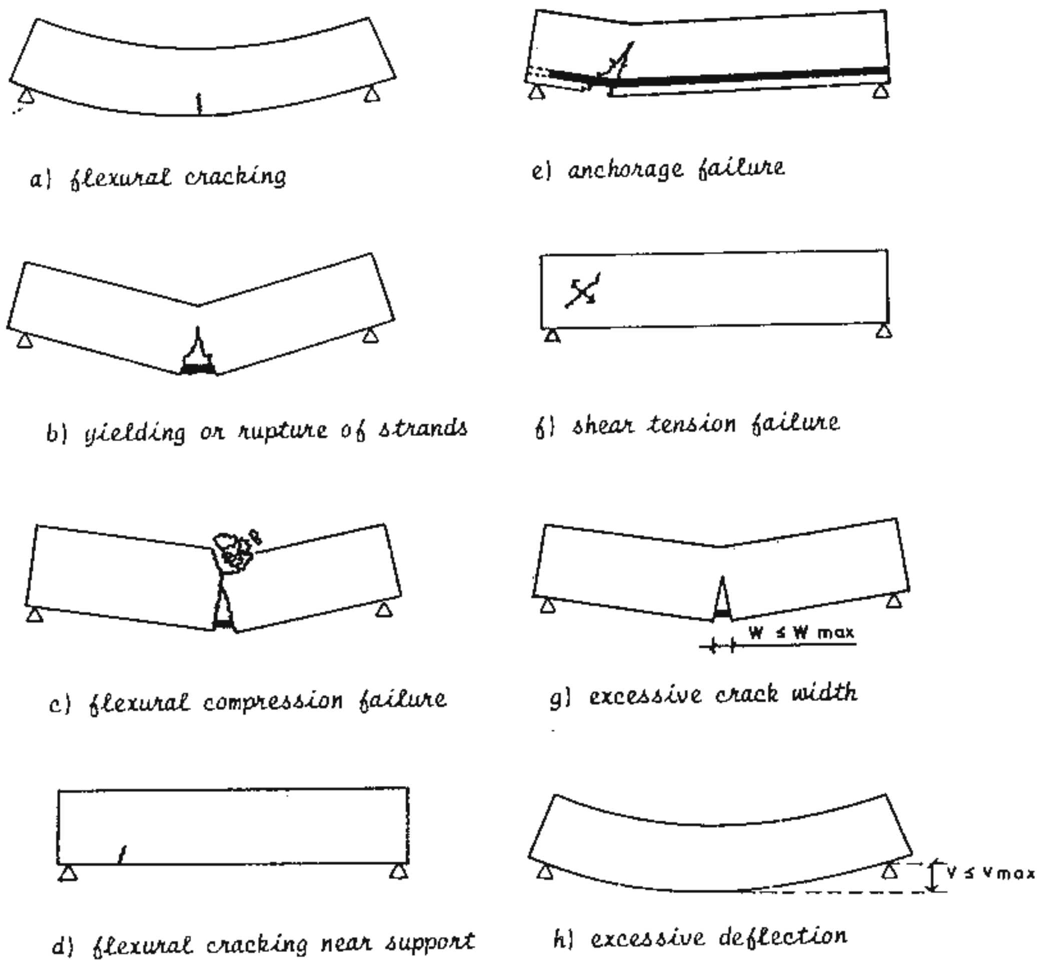

Fig. 1 Relevant limit states for a prestressed hollow core slab.

Out of these, a, b and c may be regarded as flexural ultimate limit states; d, e and f as shear ultimate limit states and a, g and h as serviceability limit states. In practice, the possible failure mechanisms a (flexural cracking) and c (flexural compression failure) are eliminated by setting a lower and an upper limit for the tensile capacity of the strands. So the flexural cracking should not limit the failure capacity. Some aspects of the other limit states are discussed below.

2.1 Flexural failure

A hollow core slab with a small number of prestressing strands loaded with nearly constant bending moment is ductile because the strands have relatively weak bond properties and hence possess a considerable elongation capacity. A slab of this type often loses its load-carrying capability due to large deflection rather than the yielding or rupture of the strands. To avoid the complicated deflection considerations for a cracked slab, for the strength of steel the 0,2% yield strength $f_{0,2}$ is used instead of the failure strength. Otherwise the flexural capacity is calculated according to /6/. The method is well-known and is therefore not repeated here.

2.2 Flexural cracking

It is common practice to assume that cracks appear at the bottom of a slab when the tensile stress calculated according to the elementary theory of bending is equal to the modulus of rupture of concrete.

A flexural crack may lead to an immediate failure if the tensile capacity of the strands is too small. To avoid this brittle failure mode, a lower limit is set for the tensile capacity of the strands. However, near the end of the slab where the anchorage capacity of the strands is not fully developed, the tensile capacity of the strands is small and if a flexural crack forms, it grows to a shear crack and an immediate failure may follow. The cracking capacity depends on the prestressing force. The curves adopted for the development of the prestressing force and anchorage capacity are illustrated in Fig. 2.

2.3 Anchorage failure

When a flexural crack near support does not lead to an immediate failure, the crack width grows until the anchorage of the strands fails (anchorage failure) or the concrete crushes on the top of the slab (shear compression failure). Since shear compression failure is preceded by remarkable bond slip, it is possible to replace the considerations concerning the shear compression failure by a proper choice of anchorage properties when the anchorage failure is considered.

Within the anchorage development area, the anchorage capacity and the flexural cracking capacity are coupled in the sense that only the greater governs the failure. If the cracking capacity of a cross section is greater, it corresponds to the failure capacity of the cross section. If the cracking capacity is smaller, a flexural crack will appear, but the cross section will not fail until the loading corresponds to the anchorage capacity.

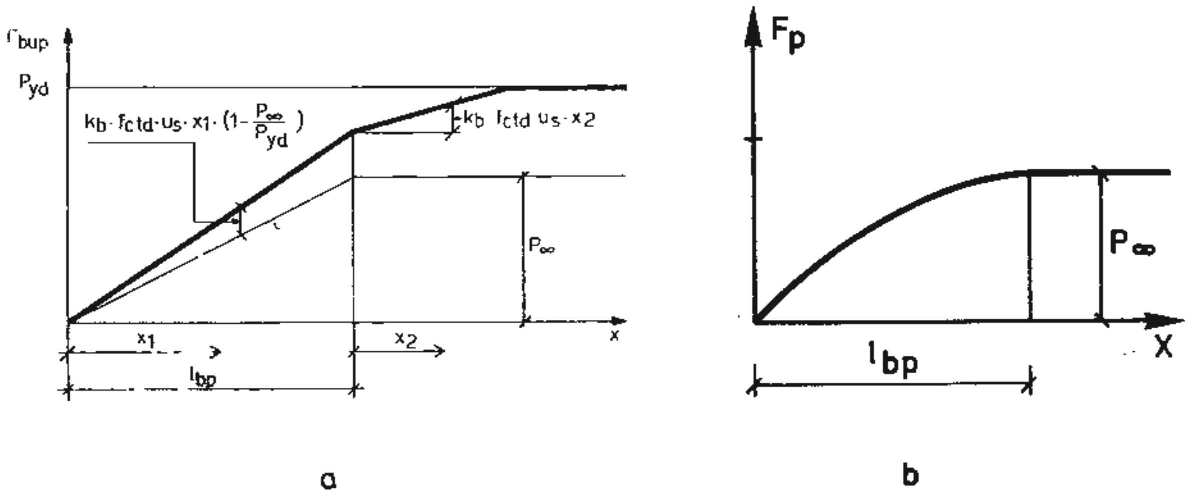

Fig. 2 . a) Development of anchorage capacity of strand .
b) Development of prestressing force.
F_{ubp} is anchorage capacity, P_{yd} ultimate capacity of strand, P_∞ fully developed prestressing force, f_{ctd} tensile strength of concrete, $u_s = \pi\phi$ and $l_{bp} = 70\phi/k_b$ where ϕ is the diameter of strand and k_b bond factor.

The same is true for the flexural cracking capacity and the flexural tensile capacity within the area where the anchorage is fully developed. Only the greater of these two capacities corresponds to the failure capacity.

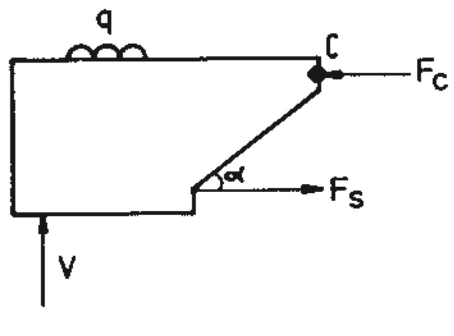

Fig. 3. Free body diagram used for calculation of anchorage capacity.

Sarja and Nykyri /2/ have proposed a method for the prediction of α. For slabs without shear reinforcement it simplifies to

$$\alpha_0 = \min(20° + (I/I_w)6°, 45°) \quad (1)$$

$$\alpha = \alpha_0 + (1 - Q_y/Q_0)(90° - \alpha) \quad (2)$$

where α_0 is the cracking angle at support, I and I_w are the second moment of inertia of the total cross section and the web, respectively, and Q_y is the shear force at distance y from support.

For Finnish prestressed hollow core slabs Eq. 1 gives 42° ... 45° for α_0. In other words, Eq. 1 could be simplified to α_0 = 45° which is commonly used for reinforced concrete. Eq. 2 means linear interpolation. At support $\alpha = \alpha_0$, at maximum bending moment α = 90°. Since the location of the critical crack is not known in advance, all possible cross sections must be checked. However, it may be concluded that the area where the anchorage is not fully developed and the area of maximum bending moment are critical. These areas are divided in small intervals and the cracking angles and capacities are calculated at the end points of these intervals. The smallest of the capacities calculated at the end points of the intervals is the failure capacity corresponding to the anchorage failure, cracking failure and yielding of strands.

2.4 Shear tension failure

When the maximum principal stress in the web of a slab reaches the tensile strength of concrete, a shear tension failure takes place. The shear force increases, the prestressing force and the support reaction decrease the maximum principal stress.The crack normally appears in the middle of the web at distance 0.5h from support, where h is the depth of the slab. It grows upwards and downwards until a wedge-formed piece is cut from the end of the slab. Since the anchorage capacity of the strands is small at support, the crack formation leads to immediate failure.

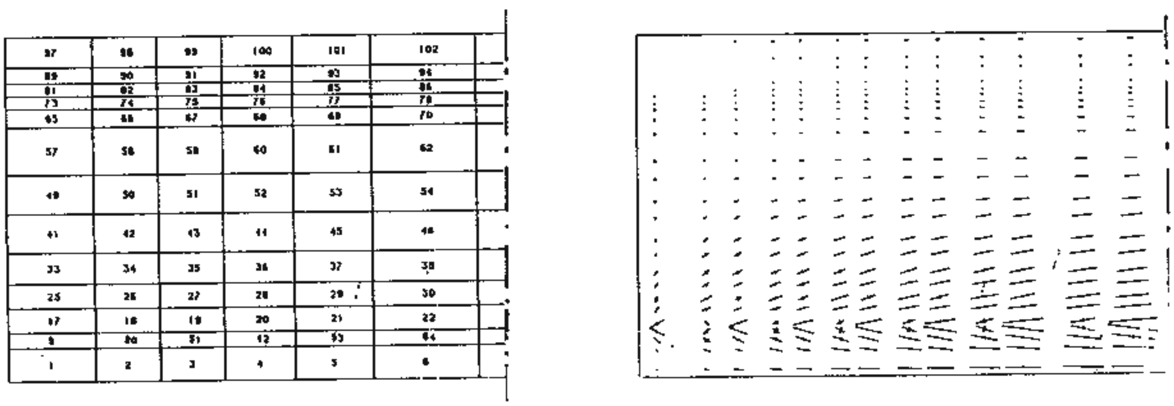

Fig. 4. The element mesh and the principal stresses due to the prestressing force at the end of a beam cut from a hollow core slab. Bernoulli's hypothesis seems to be in force.

Walraven and Mercx /3/ have proposed that the actions of the prestressing force spread in a 45° angle within the transfer length. This conclusion is based on a FEM-analysis for a rectangular prestressed beam. However, a FEM-analysis for a beam cut from a hollow core slab does not support this conclusion, see Fig. 4. According to this analysis, the elementary theory of bending can be used to predict the stresses due to the prestress and in each vertical section the prestressing force shall be taken from that very section. Hence the maximum principal stress will be

$$\sigma_{p1} = \sigma/2 + \sqrt{(\sigma/2)^2 + \tau^2} \qquad (3)$$

where τ is the shear stress due to the external loading , the normal stress σ is calculated from F/A + M/W where F is the prestressing force at distance h/2 from support, A is the area of the cross section, M is the bending moment due to F and to the external loading and W is the section modulus.

3. SIMULATION OF LOADING TESTS

To verify the design method and to check the design parameters, 298 Finnish loading tests and 42 loading tests of Jonsson /1/ were calculated by a computer program that is based on the ideas presented before.

The characteristic material properties and the geometric properties measured from the test specimens were used. Hence it is believed that if the ratio calculated / experimental capacity were smaller than or equal to one for all or almost all cases, a reasonable design system would be obtained by applying partial safety factors.

The strength of concrete used for the Finnish tests was

$$K = 1,1(C_{50}-1,65\delta) \qquad (4)$$

where C_{50} and δ are the average strength and standard deviation of the strength of the six 50 mm cylinders drilled from each slab, respectively.

The number of drilled cylinders in Jonsson's tests was so small that S could not be estimated. Therefore, a typical standard deviation for Finnish slabs, namely $0,09C_{50}$ was used.

The strength of the strands used for the Finnish slabs was 1600 MPa. For Jonsson's tests, the measured failure strengths were used but they were not critical.

Other assumptions and parameters were
- Young's modulus of strand E_p = 195000 MPa
- Development of anchorage capacity of strands and transfer of prestress according to Fig. 2

- Strength of concrete in slab $f_{ck} = 0,7K_{2/3}$
- Tensile strength of concrete $f_{ct} = 0,2K^{2/3}$
- Bond factor $k_b = 1,3$ ($k_b = \tau_b/f_{ct}$, where τ_b is the bond strength)
- Young's modulus of concrete $E_c = 4800\sqrt{K}$
- Loading age 28 d
- Creep and shrinkage parameters according to CEB-FIP model code /6/ supposing 70% relative humidity .

The geometry of the slabs as well as the experimental and calculated results cannot be included here. They are documented in a research report to be published in the near future.

3.1 Finnish quality control tests

The tests were carried out at Technical Research Centre of Finland during 1978 ... 1987. These tests belong to the quality control routine required for type approved products. All loaded ordinary prestressed hollow core slabs were included except

- slabs with excessive bond slip in one or more strands
- slabs with longitudinal cracks.

The limits for allowed bond slip were determined in accordance with the type approval requirements.

The test arrangements are shown in Fig. 5.

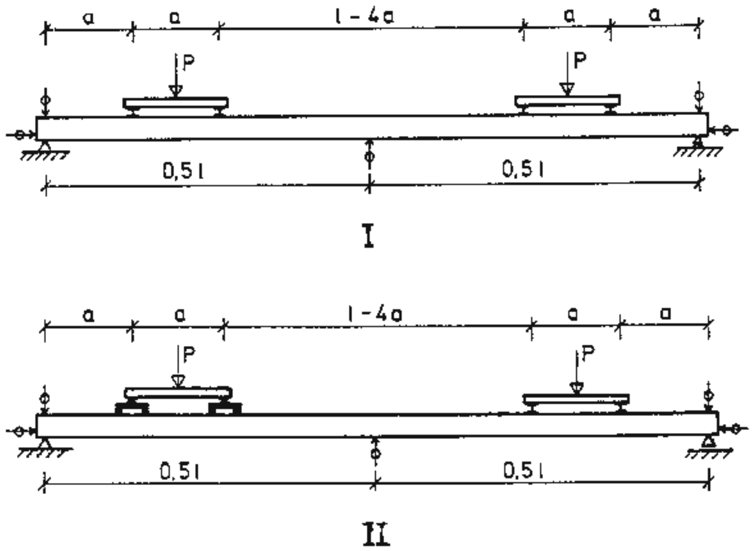

Fig. 5. Loading test arrangements. In most cases a = 1/7,2 m.

During 1985 ... 1987 a number of tests were carried out according to the system II in Fig. 7, otherwise the system I was applied. Since neither the experimental nor calculated results are sensitive to the choice of system I or II , only system I was used in calculations.

The prestress was taken from the documents of the slab producers.

The date of casting and loading was documented only for a few slabs. Hence the loss of prestress was calculated for all slabs supposing their loading age to be 28 d. In most cases the real loading age was greater.

3.1.1 Cracking capacity

The experimental cracking moment capacities correspond to the bending moment that causes 0,2 mm crack width. For some slabs, the bending moment corresponding to crack formation is also reported. From this data it can be concluded that in slabs with a small number of strands, a crack will immediately grow greater than 0,2 mm. In other words, the same bending moment corresponds to the crack formation and 0,2 mm crack width. On the other hand, if the number of the strands is great, an extra bending moment is required before a crack grows greater than 0,2 mm. This moment is typically of the order 5 ... 20 % of the bending moment corresponding to the crack formation.

The ratio modulus of rupture / tensile strength of concrete, later called relative modulus of rupture and abbreviated f_{ctfr}, was first chosen according to Mayer /7/, see Table 1. The share of slabs for which the ratio calculated / excperimental cracking moments were greater than 1,0 is also shown in Table 1.

Table 1. The relative modulus of rupture f_{ctfr} according to Mayer and the share of slabs for which the ratio predicted / observed cracking capacity was greater than 1,0.

Depth of slab mm	f_{ctfr}	Share of cases where s_c > 1,0 %
150	1,5	43
200	1,4	35
265	1,3	31
400	1,2	28

On the basis of Table 1, f_{ctfr} = 1,1 was chosen for all slabs and the results represented in Table 2 and Fig. 6 ... 9 were obtained. The probability p for the case (predicted / observed cracking capacity > 1,0) no more depends on the depth of the slab. It is also rather insensitive to the variations in the prestressing force.

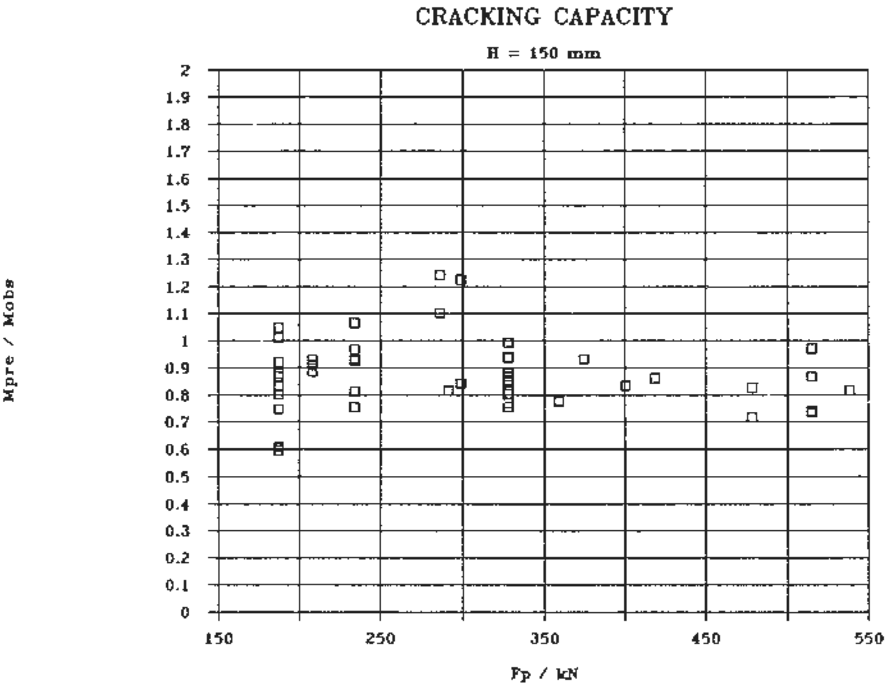

Fig. 6. The ratio predicted / observed cracking capacity for 150 mm slabs as a function of the prestressing force F_p , relative modulus of rupture = 1,1.

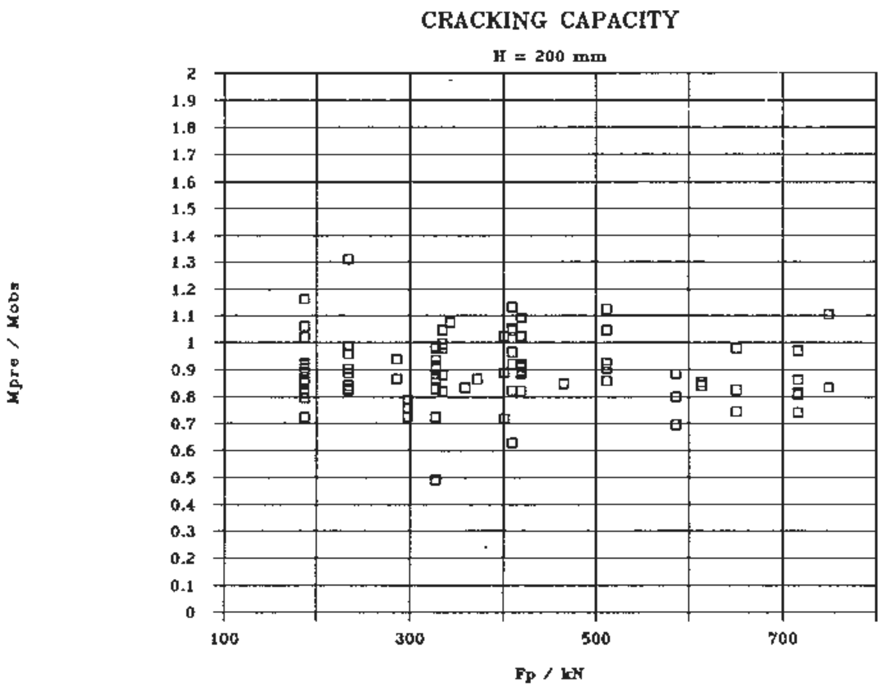

Fig. 7. The ratio predicted / observed cracking capacity for 200 mm slabs as a function of the prestressing force F_p , relative modulus of rupture =1,1.

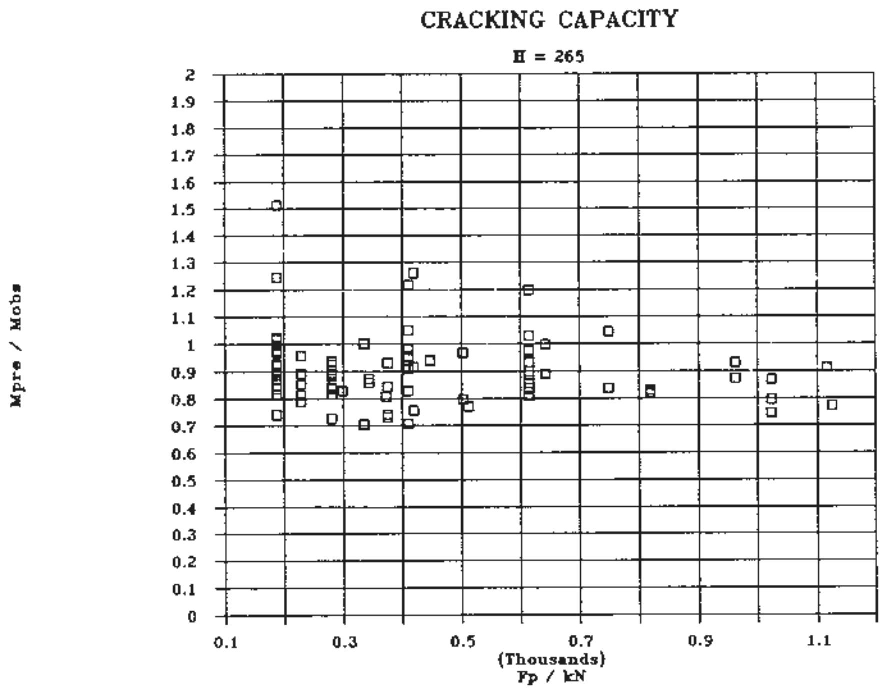

Fig. 8. The ratio predicted / observed cracking capacity for 265 mm slabs as a function of the prestressing force F_p , relative modulus of rupture = 1,1.

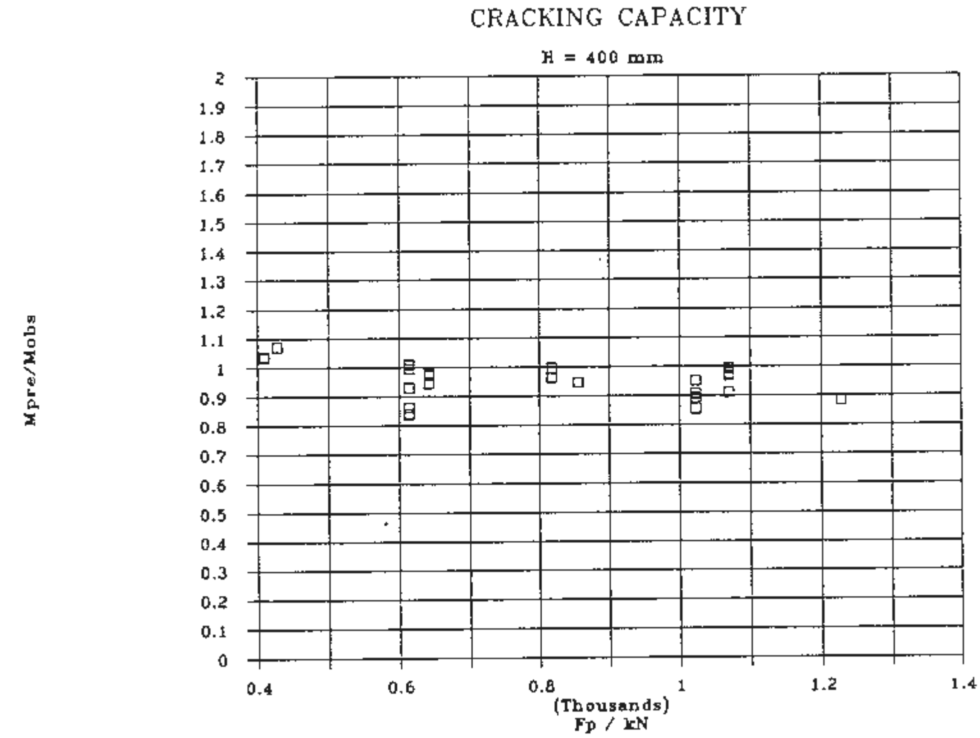

Fig. 9. The ratio predicted / observed cracking capacity for 400 mm slabs as a function of the prestressing force F_p , relative modulus of rupture = 1,1.

Table 2. Probability p for the case (predicted / observed cracking capacity > 1,0) when f_{ctfr} = 1,1.

Depth of slab mm	p %
150	17
200	19
265	22
400	18

3.1.2 Shear capacity

The failure capacity is considered in two parts: shear capacity and flexural capacity. In this context shear failure means that the failure takes place near support within the area where the anchorage capacity of the strands is not fully developed.

In Fig. 10,...,13 the ratio of calculated and experimental shear force is presented for the slabs which either experimentally or theoretically failed in shear. As can be seen, the share of points with ordinates greater than 1,0 is small for 150, 200 and 265 mm slabs and it seems justified to use this calculation method for design. On the contrary, the opposite is true for 400 mm slabs.

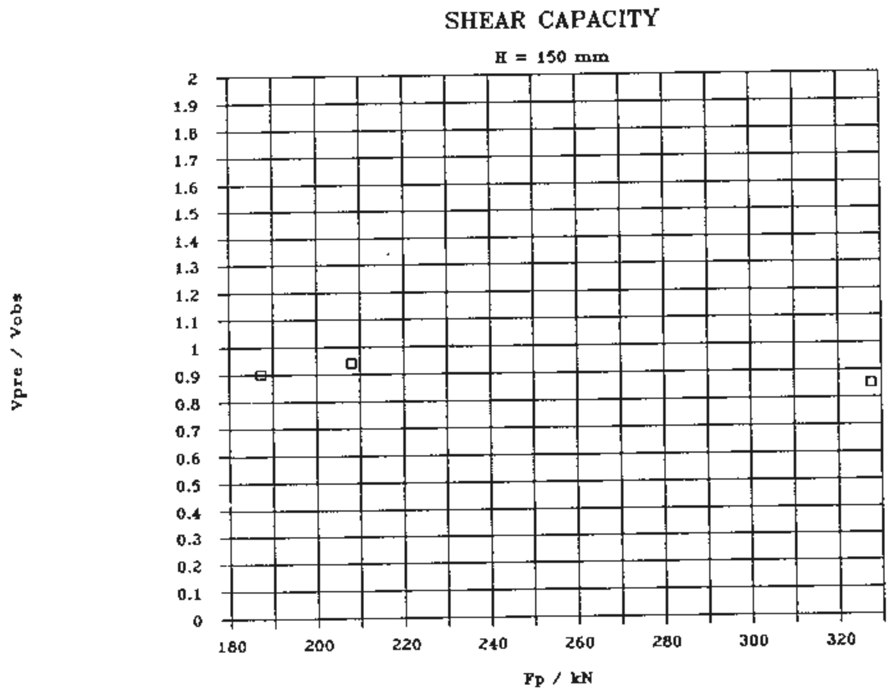

Fig. 10. The ratio predicted / observed shear capacity for 150 mm slabs as a function of the prestressing force F_p.

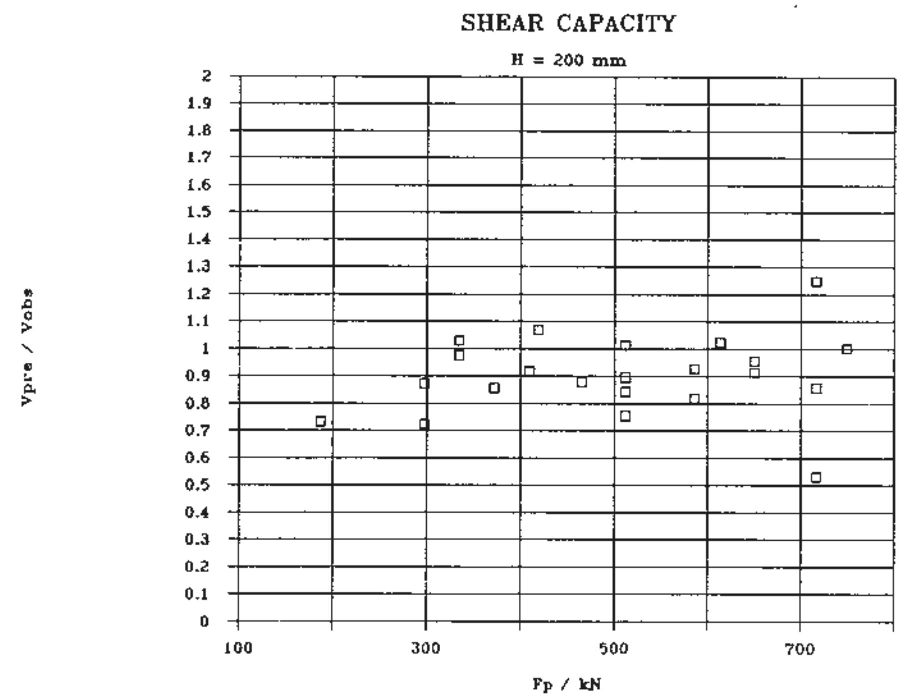

Fig. 11. The ratio predicted / observed shear capacity for 200 mm slabs as a function of the prestressing force F_p .

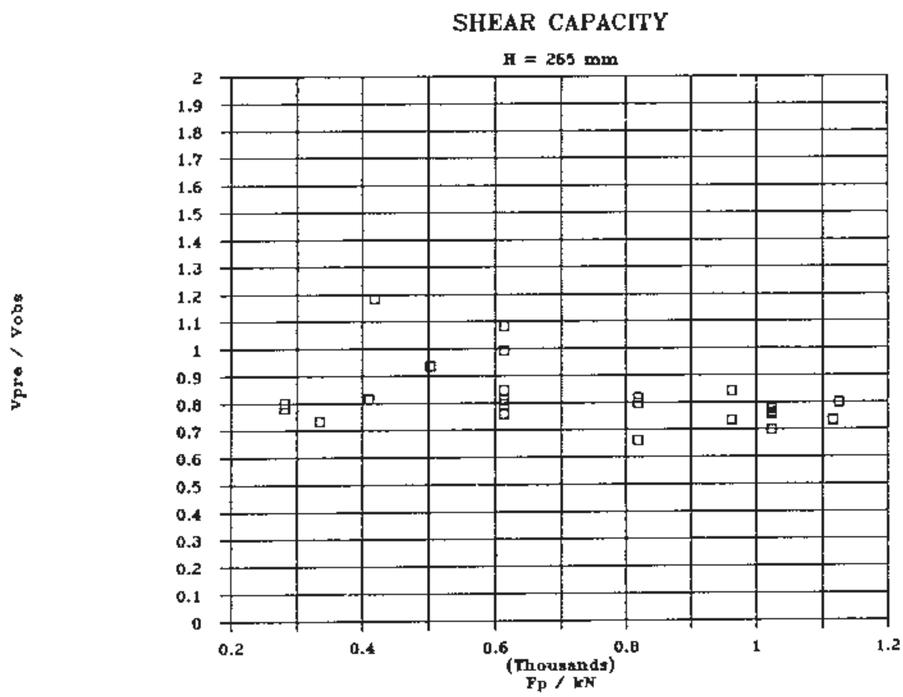

Fig. 12. The ratio predicted / observed shear capacity for 265 mm slabs as a function of the prestressing force F_p .

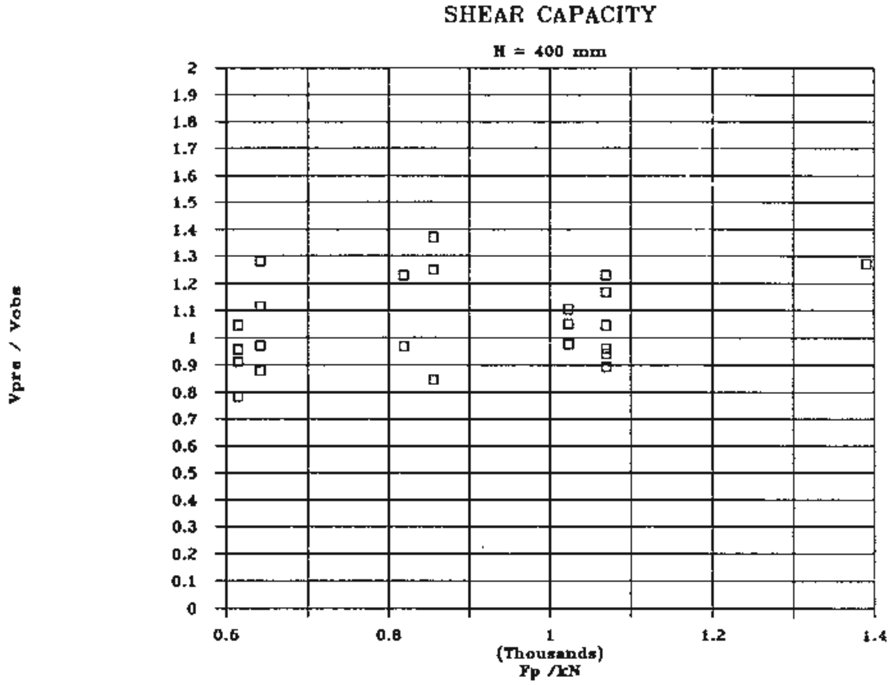

Fig. 13. The ratio predicted / observed shear capacity for 400 mm slabs as a function of the prestressing force F_p .

All the 400 mm slabs, the failure load of which was smaller than the calculated failure load, failed according to the shear tension failure mode. Hence there is something unsatisfactory in the modelling of the shear tension failure. If the theory used for the calculation of the principal stress is correct, either the prestressing force or the tensile strength of the concrete must be erroneous.

Theoretically,if the transfer rate of the prestressing force were too high at the end of the slab, the ratio calculated / experimental shear capacity would increase as the prestressing force increases. This is not the case. Therefore it is concluded that the tensile strength of concrete in the web is overestimated. The reason may be difficulties in compacting the deep and narrow web. Another reason may be that in a 400 mm slab the breadth of the web is constant and the principal stress is also nearly constant for the depth of 170 ... 210 mm which means that the critical area is essentially greater than e.g. in 265 mm slabs. Hence the risk for a brittle shear tension failure is greater for 400 mm slabs than for 265 or 200 mm slabs.

No data about the tensile strength of the web is available. A simple way to obtain reasonable results is to reduce the tensile strength of the web concrete. When a reduction factor 0,70 was used, the results expressed in Fig. 14 were obtained. It seems that this reduction factor yields shear capacities conservative enough.

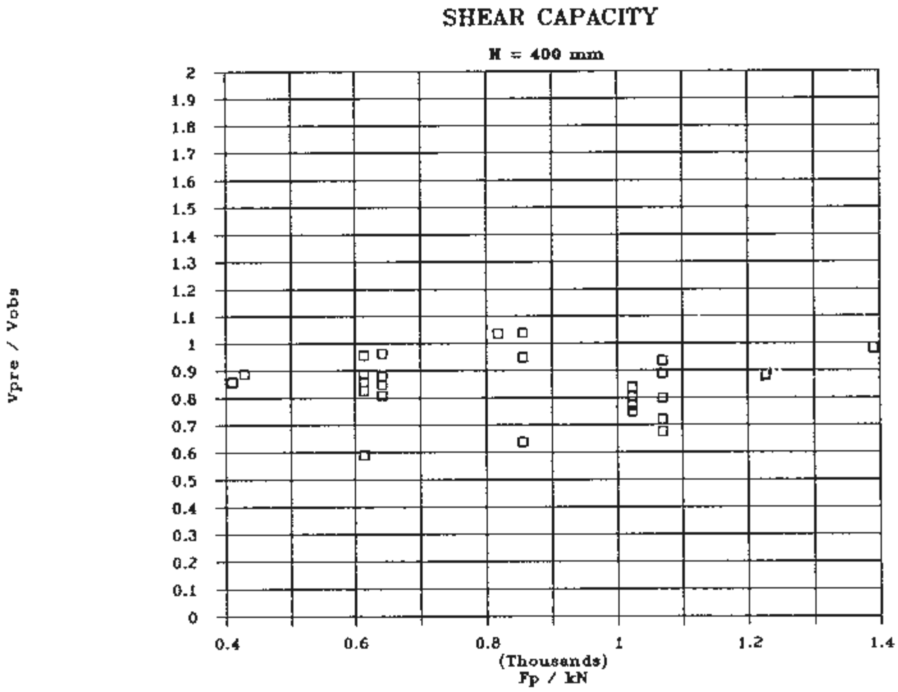

Fig. 14. The ratio predicted / observed shear capacity for 400 mm slabs as a function of the prestressing force F_p .The tensile stress in the web is 30%. reduced.

3.1.3 Flexural capacity

The probability for overestimation of the flexural capacity appeared to be smaller than five percent. Hence it can be concluded that the flexural capacity of the hollow core slabs is predicted conservatively enough when the 0,2% yield strength is used for the strands.

3.2 Jonsson's shear tests

Jonsson's test arrangements are shown in Fig. 15. His specimens were 265 mm slabs with five hollows. Nine were of the type SPENNDEKK and twelve of the type SPIROLL. The prestressing force was 475 ... 1188 kN. The ends of each slab were loaded separately, so that 42 experimental failure capacities were obtained.

The results of the calculations are shown in Fig. 16. As can be seen, they are similar to those of the Finnish 265 mm slabs. There are four points with ordinates slightly greater than 1,00. They correspond to load tests where a vertical crack, or a partly vertical, partly inclined crack formed under the load. The calculated failure mode for these four slabs was flexural cracking near support. Other slabs failed according to the shear tension failure mode both theoretically and experimentally.

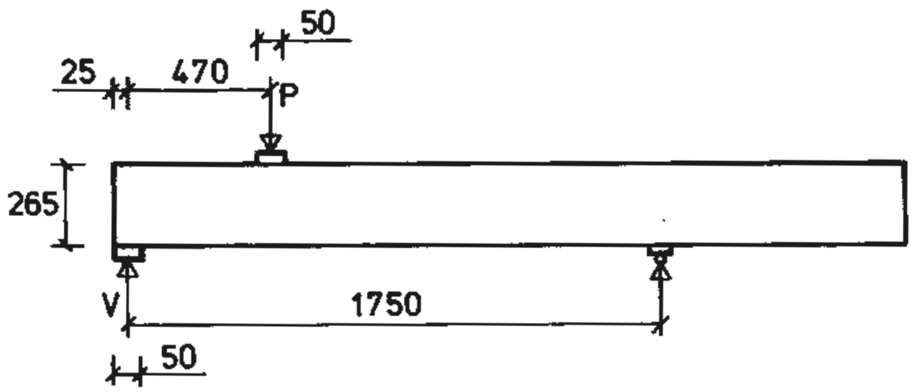

Fig. 15. Jonsson's test arrangements.

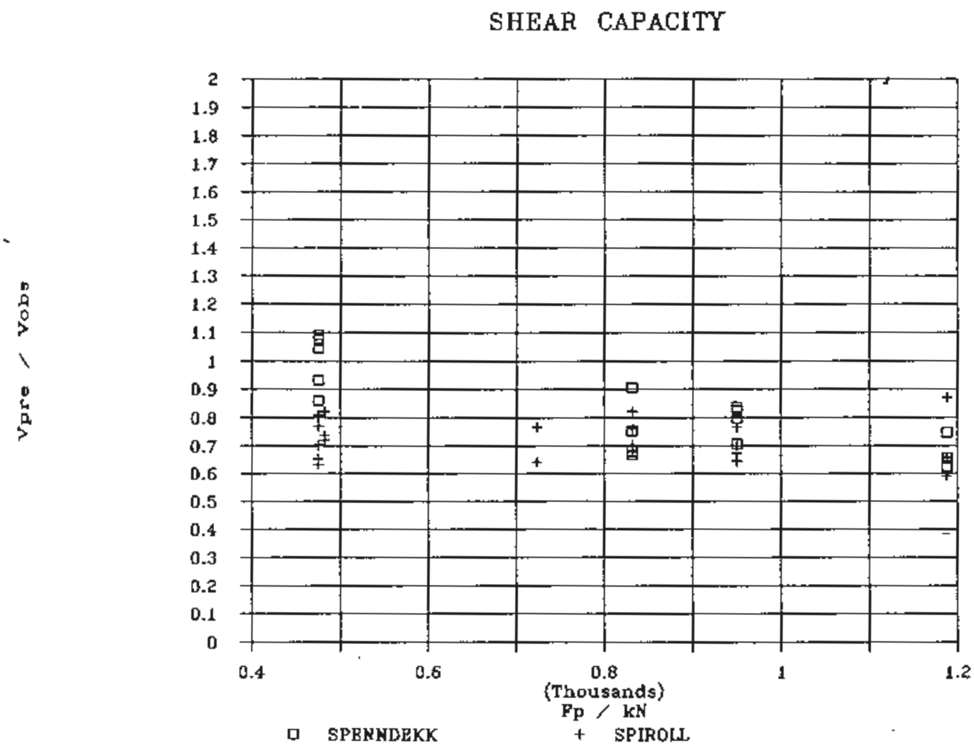

Fig. 16. The ratio predicted / observed shear capacity for Jonsson's slabs as a function of the prestressing force F_p .

4. CONCLUSIONS

The modulus of rupture seems to be insensitive to the thickness of the hollow core slab. The elementary theory of bending gives cracking moments that exceed the experimental cracking moments in 17 ... 22% of the cases when $f_{ct} = 0,2K^{2/3}$ is used for the tensile strength of concrete and the modulus of rupture is set equal to $1,1f_{ct}$. Here the experimental cracking moment corresponds to the bending moment that causes a 0,2 mm crack width. It is the same as the bending moment corresponding to the crack formation if the number of the strands is small.

There are no problems with the flexural capacity if the 0,2% yield strength is used for the strength of the strands. On the contrary, the flexural capacity may be overestimated if the failure strength is used for the strands.

The shear tension failure can be modelled by comparing the maximum principal stress in the web to the tensile strength of concrete. The maximum principal stress is calculated at the distance h/2 from the support, where h is the depth of the section. When calculating the maximum principal stress, the shear stress due to the external load and the normal stress due to the prestressing force must be taken into account but the bending stresses due to the prestressing force and external bending moment are of minor importance. When calculating the normal stress, the elementary theory of bending is used and the prestressing force is taken from the same vertical section where the principal stress is to be calculated. The tensile strength of concrete may vary within a slab. It turned out that the strength based on specimens drilled from the top of the slab gave good results for the shear tension capacities of the 200 mm and 265 mm slabs but had to be reduced by 30% for the 400 mm slabs.

The design against the shear compression failure mode can be covered by the design against the anchorage failure mode. This conclusion is also supported by the results of Walraven and Mercx /3/. If they had not considered the shear compression failure, their calculated and experimental shear capacities would have agreed better than they have reported.

Since the failure and cracking capacities of a prestressed hollow core slab can be predicted with reasonable reliability, a satisfactory design method is obtained by applying proper safety factors for the loads and material properties.

5.REFERENCES

/1/ Jonsson, E., Shear capacity of prestressed hollow-core slabs. Nordisk Betong, 4-1980, pp. 27-31.

/2/ Sarja, A. & Nykyri, P., Rotational model for the determination of the shear capacity of reinforced and prestressed concrete structures. Technical Research Centre of Finland. Research reports 76, Espoo 1982. 19 p.

/3/ Walraven, J.C. & Mercx, W.P.M., The bearing capacity of prestressed hollow core slabs. Heron, vol. 28 no. 3, 1983.
46 p.

/4/ Becker, R.J. & Buettner, D.R., Shear tests of extruded hollow-core slabs. PCI Journal, March-April 1985. pp. 41-51.

/5/ Buettner, D.R. & Becker, R.J., PCI manual for the design of hollow core slabs. PCI, Chicago, Illinois 1985. 114 p.

/6/ CEB-FIP model code for concrete structures. Comité Euro-International du Béton, 1978. 348 p.

/7/ Mayer, H., Die Berechnung der Durchbiegung von Stahlbetonbauteilen. Deutscher Auschuss für Stahlbeton, Heft 194, Berlin 1967. 73 p.